The role of the tongue-of-ionization in the formation of the poleward wall of the main trough in the European post-midnight sector

H. R. Middleton,[1] S. E. Pryse,[1] A. G. Wood,[1] and R. Balthazor[2,3]

Received 6 July 2007; revised 24 August 2007; accepted 17 October 2007; published 16 February 2008.

[1] A series of radio tomography reconstructions from the University of Wales Aberystwyth receiver chains in Scandinavia and the UK, imaging the midnight-dawn sector on 13 December 2001, reveal a persistent large-scale electron density enhancement, which forms the poleward wall of the main ionization trough. Measurements by the European Incoherent Scatter radar (EISCAT) rule out in situ soft-particle precipitation as the main source of the higher densities. SuperDARN plasma drift observations and electric potential patterns place the feature in the dawn cell of the high-latitude convection, leading to the conclusion that the higher density is likely to have originated as photoionization and was convected over the polar cap to the nightside and around toward dawn in a tongue-of-ionization (TOI). Suitable runs of the Coupled Thermosphere-Ionosphere-Plasmasphere (CTIP) model support this interpretation and also reveal that the formation of the TOI is heavily UT dependent, which would lead to it being most prominent at nighttime in the European sector.

Citation: Middleton, H. R., S. E. Pryse, A. G. Wood, and R. Balthazor (2008), The role of the tongue-of-ionization in the formation of the poleward wall of the main trough in the European post-midnight sector, *J. Geophys. Res.*, *113*, A02306, doi:10.1029/2007JA012631.

1. Introduction

[2] The plasma in the ionosphere is structured spatially on a wide range of horizontal scale sizes and can demonstrate significant temporal variation. The main ionospheric trough is a persistent large-scale depletion in *F* region ionization, typically present through the post-afternoon to dawn sector (18-06 MLT)[*Kersley et al.*, 1997], separating the auroral and midlatitude regions (see reviews by *Rodger et al.*, 1992; *Moffett and Quegan*, 1983). Although mainly observed between dusk and dawn, it can extend into the afternoon sector at high latitudes and is generally seen to move to lower latitudes with increasing local time and geomagnetic activity. Around dawn, the depletion is 'filled in' by the photoionization of the new day. The morphology of the trough is important to the understanding of the geophysics of the interface between the mid- and high-latitude ionosphere and accurate prediction of the location of the trough is important in areas such as trans-ionospheric communication and navigation systems, where the steep gradients of the walls of the trough can affect performance.

[3] The main trough has been studied since its discovery from topside soundings in the sixties [*Muldrew*, 1965] but the mechanisms behind the production and maintenance of the trough and the walls flanking it are not completely certain and the poleward wall has had little attention, particularly in the midnight-dawn sector. Pre-midnight and pre-Harang discontinuity (evening sector), the production of the depletion forming the trough has been attributed to several different mechanisms. One of these is stagnation and decay of ionization in darkness in the region where high-latitude convection and corotation counter each other [e.g., *Knudsen*, 1974; *Collis and Häggström*, 1988]. Another proposed production mechanism of the depletion are sub-auroral ion drift (SAID) events where enhancement in electric field cause high-speed ion flow confined to a narrow band of latitudes, but extended in longitude, and consequently cause associated depletions in electron concentration due to increased recombination rate [*Rodger et al.*, 1992 and references therein].

[4] Post-midnight, it has been suggested that transport and precipitation are the significant factors in forming the trough, although *Rodger et al.* [1986] proposed that transport was the more important mechanism. The 'fossil' mechanism, proposed by *Evans et al.* [1983], is another possibility where a depletion formed in the dusk side, as a result of a substorm, then corotates into the nightside sector toward dawn. However, in the review by *Rodger et al.* [1992], it was pointed out that the trough at these local times might just be the 'normal' ionosphere between two enhancements, where the poleward wall is formed in situ by precipitation or transported from elsewhere and the equatorward wall is the decaying photoionization corotating into the midnight-dawn sector. Hence the mechanisms involved may be more cases of reconfiguration of ionization

[1]Institute of Mathematical and Physical Sciences, University of Wales Aberystwyth, Aberystwyth, United Kingdom.
[2]US Air Force Academy, Department of Physics, Colorado Springs, Colorado, USA.
[3]Formerly at Space Physics and Upper Atmosphere Research Group, Department of Applied Mathematics, University of Sheffield, Sheffield, United Kingdom.

0148-0227/08/2007JA012631

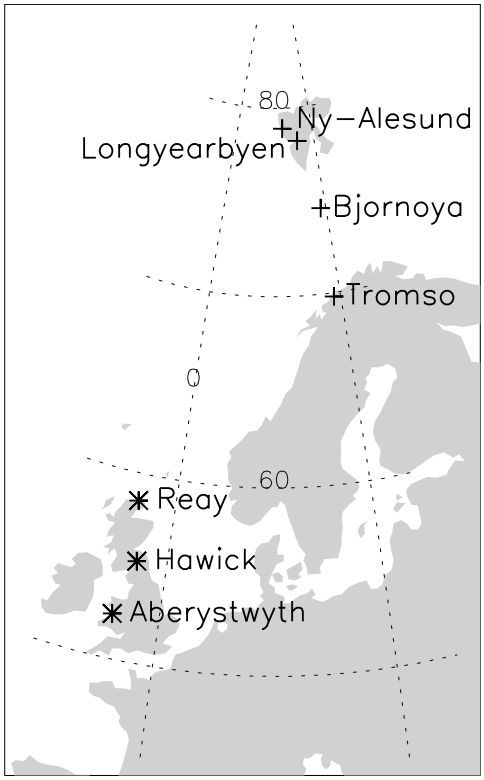

Figure 1. Map of radio tomography receiver stations in Norway and UK.

already present or precipitation forming the walls rather than the decay of ionization to form the trough.

[5] There have been a few attempts to build empirical formulae for predicting the location of the main trough [e.g., *Rycroft and Burnell*, 1970; *Collis and Häggström*, 1988]. Tomography has been used in a recent study to parameterise the location and shape of the trough at midlatitudes over the UK [*Pryse et al.*, 2006a]. Obviously, both empirical and numerical models are important for predicting the structure of the ionosphere and neither can be used with any reliability if they haven't been verified by comparison with observations [e.g., *Pryse et al.*, 2005].

[6] Tomography is a particularly useful tool for investigating features on the scale-size of the trough. It can observe the spatial electron density distribution on a 2D plane on scales of tens to hundreds of kilometers [see *Pryse*, 2003 and references therein]. The case study in this paper uses a series of tomographic reconstruction images observed on the night of the 12–13 December 2001 and CTIP model predictions to show that on this occasion, the poleward edge of the main trough in the midnight-dawn sector is most likely photoionization that has convected over the pole and around toward dawn. Observations from EISCAT and SuperDARN further support this interpretation.

2. Instrumentation and Model

2.1. Radio Tomography

[7] Ionospheric radio tomography uses radio transmissions from polar-orbiting satellites and a chain of ground receiver stations to produce maps of the electron density distribution in a latitude-altitude plane. The Navy Ionospheric Monitoring Systems (NIMS) satellites, formerly Navy Navigation Satellite System (NNSS), are used as they are in low polar orbits. These satellites transmit two phase-coherent signals at 150 and 400 MHz. The phase difference between these two signals when received at the ground station enables the measurement of the line integral of electron density, the total electron content (TEC), along the satellite-to-receiver raypath. Each station thereby builds a profile of the TEC over the course of the satellite's path. The chain of stations is positioned along a line of longitude, separated in latitude and therefore measurements are made along a large number of intersecting paths. Tomographic inversion of the data yields a 2D map of the electron density spatial distribution over hundreds of kilometers. The technique gives accurate latitudinal distribution within the latitude range of the receivers; however, the lack of horizontal raypaths means that the determination of the vertical distribution of ionization is not so reliable [e.g., *Raymund et al.*, 1994]. We would therefore advise slight caution or turn to other instruments to verify the altitudes of important features.

[8] At the time of these observations, the University of Wales Aberystwyth ran two radio tomography chains: one in Scandinavia and the other in the UK (see Figure 1). The Scandinavian chain consists of receivers at Ny-Ålesund (78.9°N, 12.0°E) and Longyearbyen (78.2°N, 15.7°E) on Svalbard, Bjørnøya (Bear Island; 74.5°N, 19.0°E) and Tromsø on mainland Norway (69.8°N, 19.0°E). The UK chain consisted of stations at Reay (58.6°N, −3.8°E), Hawick (55.4°N, −2.8°E) and Aberystwyth (52.4°N, −4.1°E).

2.2. CTIP Model

[9] Sheffield University and University College London (UCL) developed the Coupled Thermosphere-Ionosphere-Plasmasphere (CTIP) model from a thermospheric model [*Fuller-Rowell and Rees*, 1980, 1983] and a plasmasphere and high-latitude ionospheric model with plasma convection and precipitation energy inputs [*Quegan et al.*, 1982]. Various adaptations of the code have been carried out: the version used in this study is the Sheffield University CTIP model. Coupled equations of momentum, energy and continuity are solved on a geocentric grid and outputs of ion and neutral densities, velocities and temperatures are produced. Only the ion density results are used in this study.

[10] The model was run for conditions closest to those on the day of observation: the day number was set to 347 (13 December) and the F10.7 index to 230. The precipitation energy input, which is set according to the classification of DMSP satellite measurements by *Hardy et al.* [1985], was set to a K_p level of 2 to match the conditions on the day. The convection input is in the form of 37 electric potential patterns taken from Millstone Hill convection models [*Foster et al.*, 1986]; number 33 was chosen and is shown in Figure 2. This convection pattern was chosen because it is the nearest to representing the conditions of negative interplanetary magnetic field (IMF) By and Bz which were prevalent at the time of observation (see IMF conditions, Figure 3). This convection pattern was used for the entire

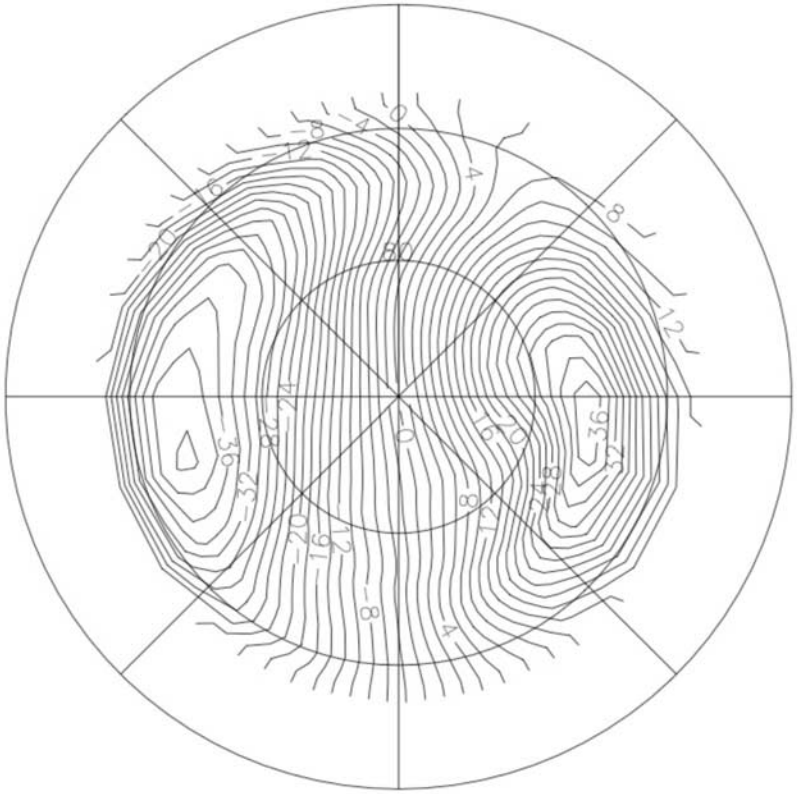

Figure 2. Map of electric potential (in kV) used in CTIP model run on a MLT versus magnetic latitude polar plot. Magnetic local noon is at the top of the figure, 06 MLT on the right hand side, 18 MLT on the left hand side and the latitude increments are in 10 degrees from 60 degrees MLAT on the outer circumference to 90 degrees MLAT at the centre. The positive potential is on the dawn side.

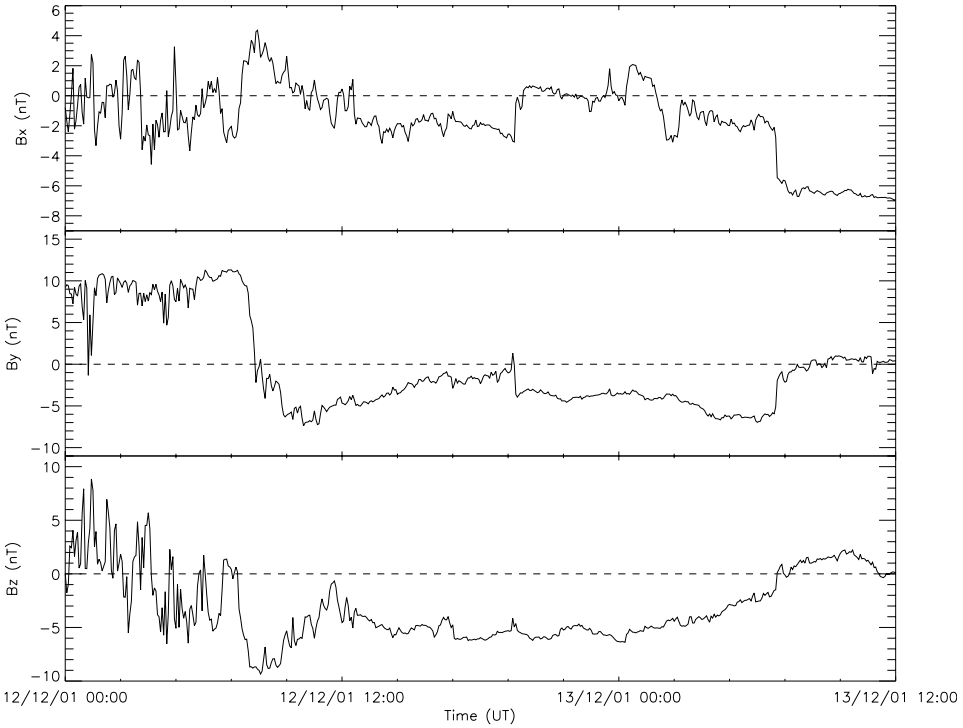

Figure 3. Interplanetary magnetic field measured by the ACE satellite from 00 UT on 12 December 2001 to 12 UT 13 December 2001.

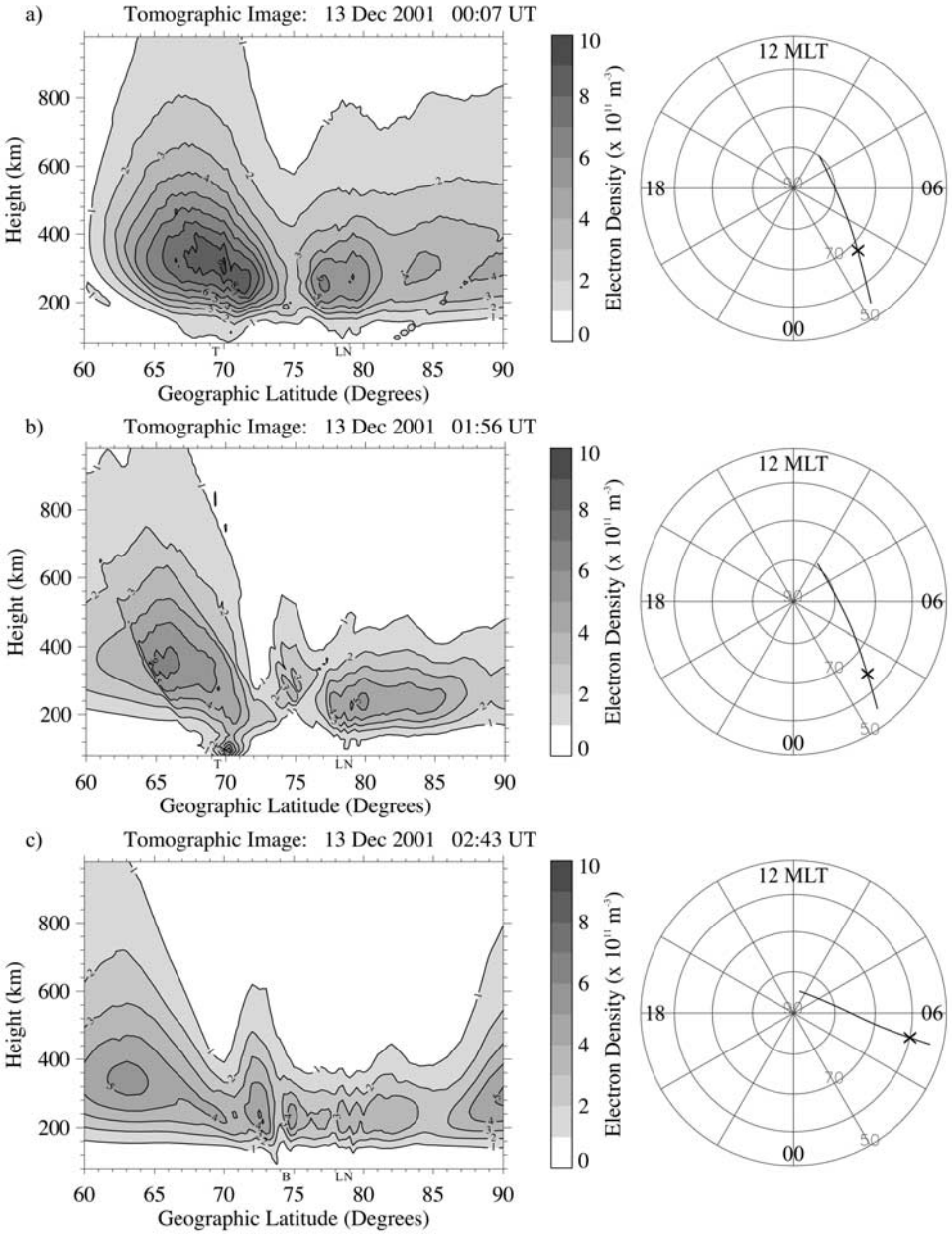

Figure 4. Scandinavian chain reconstructions and satellite 350 km intersection trajectories. The letters under the *x* axis show the locations of the receiving stations involved in the reconstruction. The cross superimposed on the trajectory is the approximate location of the center of the electron density enhancement.

model run which ran for 8 days and the final complete day was used in this study.

3. Observations

3.1. Interplanetary Magnetic Field

[11] The interplanetary magnetic field measured upstream in the solar wind by the Advanced Composition Explorer (ACE) satellite is shown for 00 UT 12 December 2001 to 12 UT on 13 December 2001 in Figure 3. Allowing for the delay, both the By and Bz components were consistently negative throughout the observing period (2305 UT on 12 December 2001 to 0234 UT on 13 December 2001; see tomographic reconstructions, Figures 4 and 5) and had been so for more than 10 h before the first observation. This stability is helpful in ensuring a relatively unchanging ionosphere for the duration of the observations. This also helps in the choice of electric potential pattern for the CTIP model as at present the current version takes one convection pattern for the whole run.

3.2. Radio Tomography

[12] The tomographic observations made with the Scandinavian chain are shown in Figure 4. In each panel of the figure, the tomographic image on the left shows electron density as a function of latitude and altitude, and the

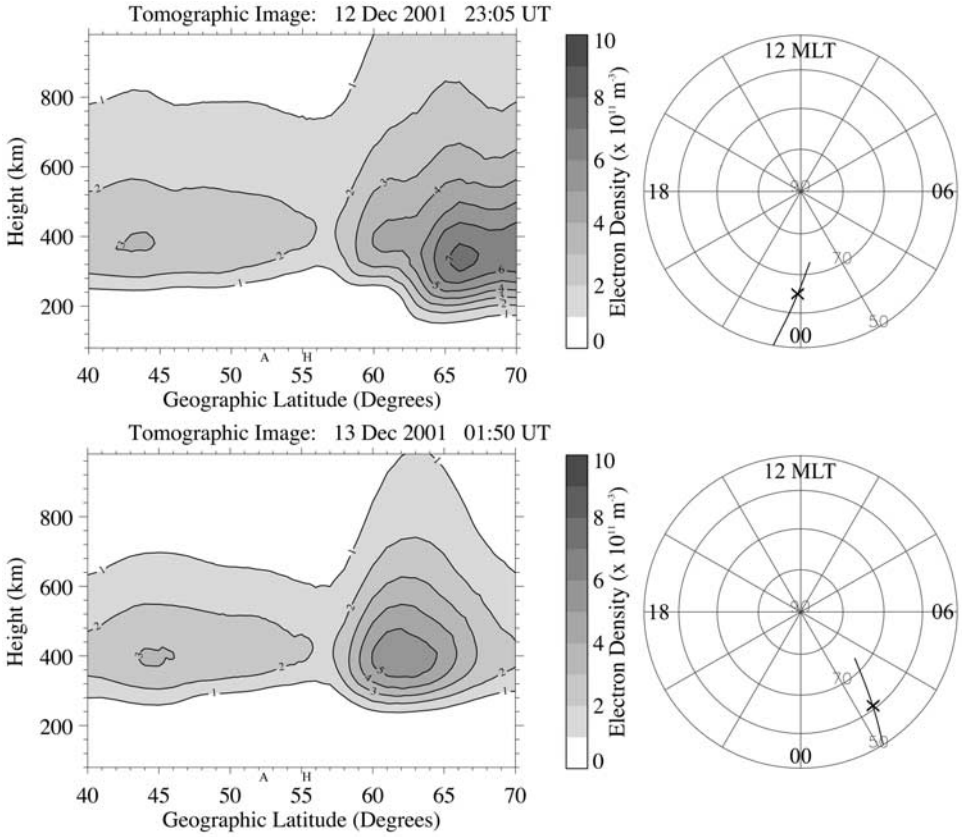

Figure 5. UK chain reconstructions and satellite 350 km intersection trajectories. The letters under the *x* axis show the locations of the receiving stations involved in the reconstruction. The cross superimposed on the trajectory is the approximate location of the peak of the electron density enhancement.

diagram on the right presents the path of the satellite 350 km intersection on a geomagnetic latitude and magnetic local time (MLT) polar plot with 12 MLT at the top. The placement of the satellite intersection trajectory can be approximated to the location of the 'ionospheric slice' from which the densities are measured.

[13] The first observation taken at 0007 UT on 13 December 2001 (Figure 4a) shows an area of large enhanced densities up to 8×10^{11} m^{-3} between about 63 and 73 degrees north (61 and 71 degrees MLAT; limits taken at 4×10^{11} m^{-3}). The trajectory diagram places the observed plane mainly in the midnight-dawn sector, with the higher latitudes being slightly sunward of 06 MLT. The enhancement therefore is positioned with its peak at approximately 68 degrees MLAT and 3.0 MLT and is marked by the cross on the trajectory in Figure 4a.

[14] The enhancement is still present in the next observation from the Scandinavian chain taken at 0156 UT (Figure 4b). Peaking at a slightly lower level of 6×10^{11} m^{-3}, it spans 63°N to 71°N (61.4 to 69.3 MLAT) with its center at 66°N, 64.4 MLAT and 3 MLT. The line of discontinuity on the left hand side within the image is due to edge effects in the data where a station, Tromsø in this case, loses the signal of the satellite. Although the peak occurs on the edge of the available data and the image shows the transition back to the background model, the larger densities are definitely present.

[15] There is still a discernable enhancement in the observation taken at 0243 UT (Figure 4c), which the trajectory shows to be placed near magnetic dawn. The peak is 5×10^{11} m^{-3} at about 63°N, 59.9 MLAT and 5.2 MLT.

[16] The UK chain is at lower latitudes but the field-of-view extends into that of the Scandinavian chain and in this case, also into the range of the enhancement of interest. The observations from the UK chain are shown in Figure 5, along with the 350 km intersections of the trajectories of the satellite passes. The images presented here are at 2305 UT on the 12 December 2001 (Figure 5a), an earlier pass than any of the Scandinavian observations and 0150UT on the 13th, which is actually from the same satellite pass as the Scandinavian chain's observation at 0156UT. Obviously seen toward the north of the observing range, the region of higher densities is situated north of 60°N in the pass at 2305, with the peak of 7×10^{11} m^{-3} at 66°N, 65.1 MLAT and 23.9 MLT. The later UK pass at 0150 UT shows the peak to be 5.5×10^{11} m^{-3} positioned at 62°N, 61 MLAT, 2.5 MLT broadly in agreement with the Scandinavian chain's observation of the same pass. For this particular pass, the UK chain's measurements cover the peak completely while only the station at Tromsø observes the enhancement for the Scandinavian chain and therefore the position of the peak given in Figure 5b is likely to be the better determined of the two.

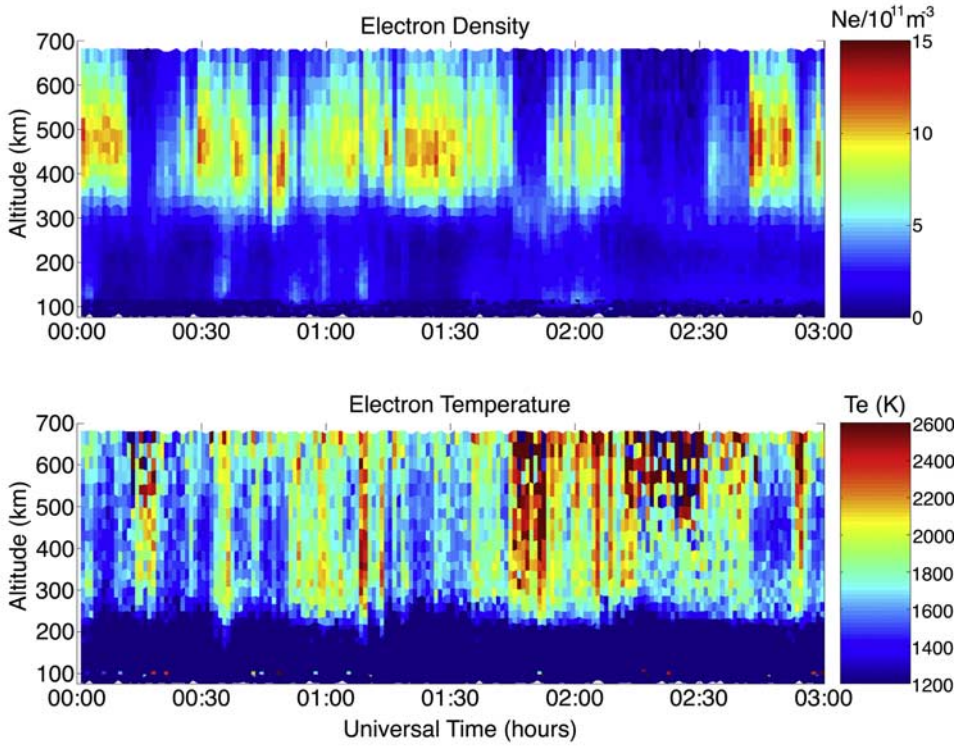

Figure 6. Electron density and temperature measured by the mainland EISCAT UHF radar between 00 UT and 03 UT on 13 December 2001.

[17] These observations, when taken together under the stable geophysical conditions, must either show a detached region of higher densities caught at these different times and positions by the tomography slices or, more likely, a continuous 'tongue' of higher ionization levels joined together, with the observations being cross sections through it.

3.3. EISCAT Observations

[18] The European Incoherent Scatter radar (EISCAT) provided continuous measurements of the ionosphere above Scandinavia throughout the time period of interest. Figure 6 presents the results from the EISCAT mainland UHF radar at Tromsø directed along the geomagnetic field at −176.7° azimuth and 77.1° elevation. The upper panel shows the electron density from 00 UT to 03 UT and the lower panel shows the electron temperature over the same time period. The electron densities reveal persistent large densities at 68.9° N, 19.1° E geographic (66.3 MLAT, 103.6 MLON) collocated with the enhancement seen in the tomographic reconstructions. This ionization is at a high altitude with a peak density at altitudes above 400km and reveals a patchy temporal variation, which is possibly due to the TOI drifting in and out of the limited field-of-view of the radar or modulation of the continuous tongue. The density is anti-correlated with the electron temperatures shown in the lower panel; the correlation between the electron density and the electron temperature at 450 km is −0.58. The height of the large densities together with the lower electron temperatures infer that the ionization is old and long-lived, with ionization which might have existed at lower altitudes having been eroded due to increased recombination where collision rates are higher. It is therefore likely that the larger densities were transported from elsewhere and not created in situ at the location of observation by particle precipitation. This provides further support for the source of this enhancement

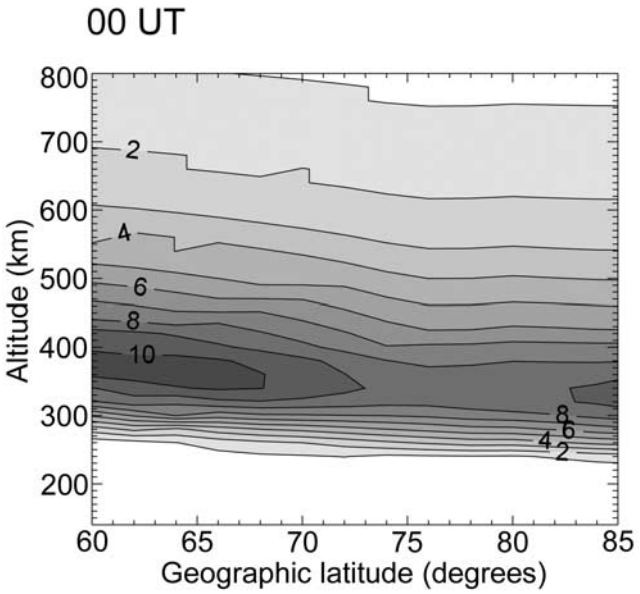

Figure 7. CTIP model results for 00 UT, 18 degrees geographic longitude for the same geographic latitude as the Scandinavian tomographic reconstructions.

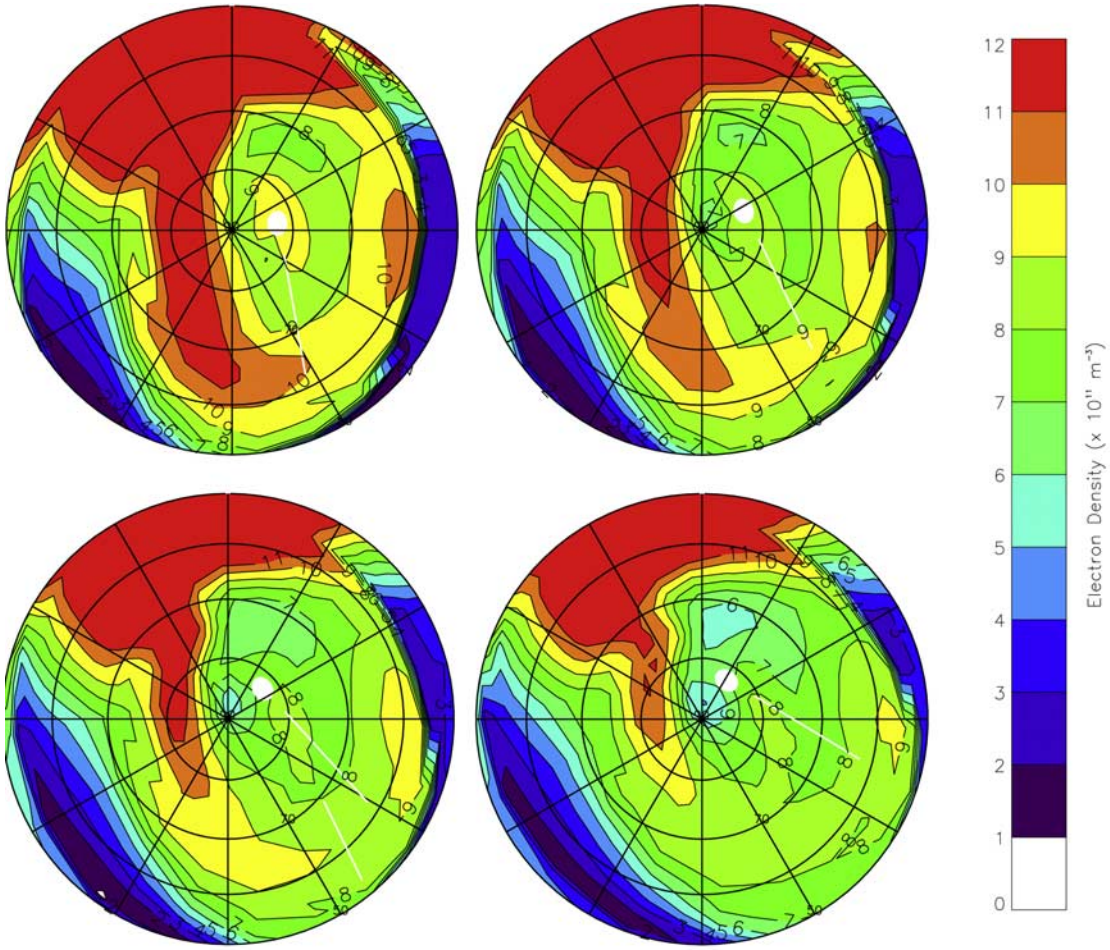

Figure 8. CTIP model results at hourly intervals between 00 and 03 UT (00 and 01 in upper panel and 02 and 03 on lower panel) for run with convection and precipitation both turned on. The latitude scale extends from 50 degrees MLAT at the edge to the geomagnetic pole at the centre. 12 MLT is at the top of each plot, with 06 MLT on the right hand side and 18 MLT on the left hand side. The single white line on most plots shows the approximate location of the Scandinavian tomography chain and the second, smaller white line on the 02 UT plot (near the time of the second UK tomography image) marks the approximate location of the UK chain.

being upstream, most likely photoionization on the dayside, which has been transported over the pole by the convection.

4. CTIP Model Predictions

[19] To obtain a better understanding of the origin of the ionization, the CTIP model was run for similar conditions as for the night of observation. Figure 7 shows the ion density output in a latitude versus altitude plot for 00 UT for 18 degrees longitude and 60–85 degrees latitude, for direct comparison with the Scandinavian tomography results. The peak of the enhancement in the plot for 00 UT is 10×10^{11} m^{-3}, which is slightly above the 8×10^{11} m^{-3} level found in the 0007 UT plot from the Scandinavian chain (Figure 4a), but the two results are remarkably similar. 00 UT is shown here in Figure 7 as an example of how the latitude versus altitude plots of the model data agree with the observations. The remaining times in this series (01–03 UT) are very similar.

[20] Figure 8 shows the ion density output at 350 km altitude plotted on MLAT versus MLT polar plots at one-hour intervals between 00 and 03 UT, covering the time period of the reconstructions when Scandinavia was in the midnight-dawn sector. Magnetic noon is at the top of each plot and the latitude scale is in increments of 10 degrees from 50 degrees MLAT at the edge to 90 degrees MLAT in the centre. The white circle near the center of the plot is the geographic pole where the model makes no predictions because of the converging lines of longitude. The white line shown on each plot shows the 18° geographic meridian between 65 and 85 °N and represents the approximate location of the Scandinavian chain, and is the longitude shown in the plot in Figure 7.

[21] The dark area to the top left of each plot in Figure 8 is clearly the photoionization, elongated slightly to the east due to co-rotation. The next most obvious feature of the figure is the tongue-of-ionization (TOI) drawn over the dusk side of the magnetic pole. At 00 UT (top left plot in

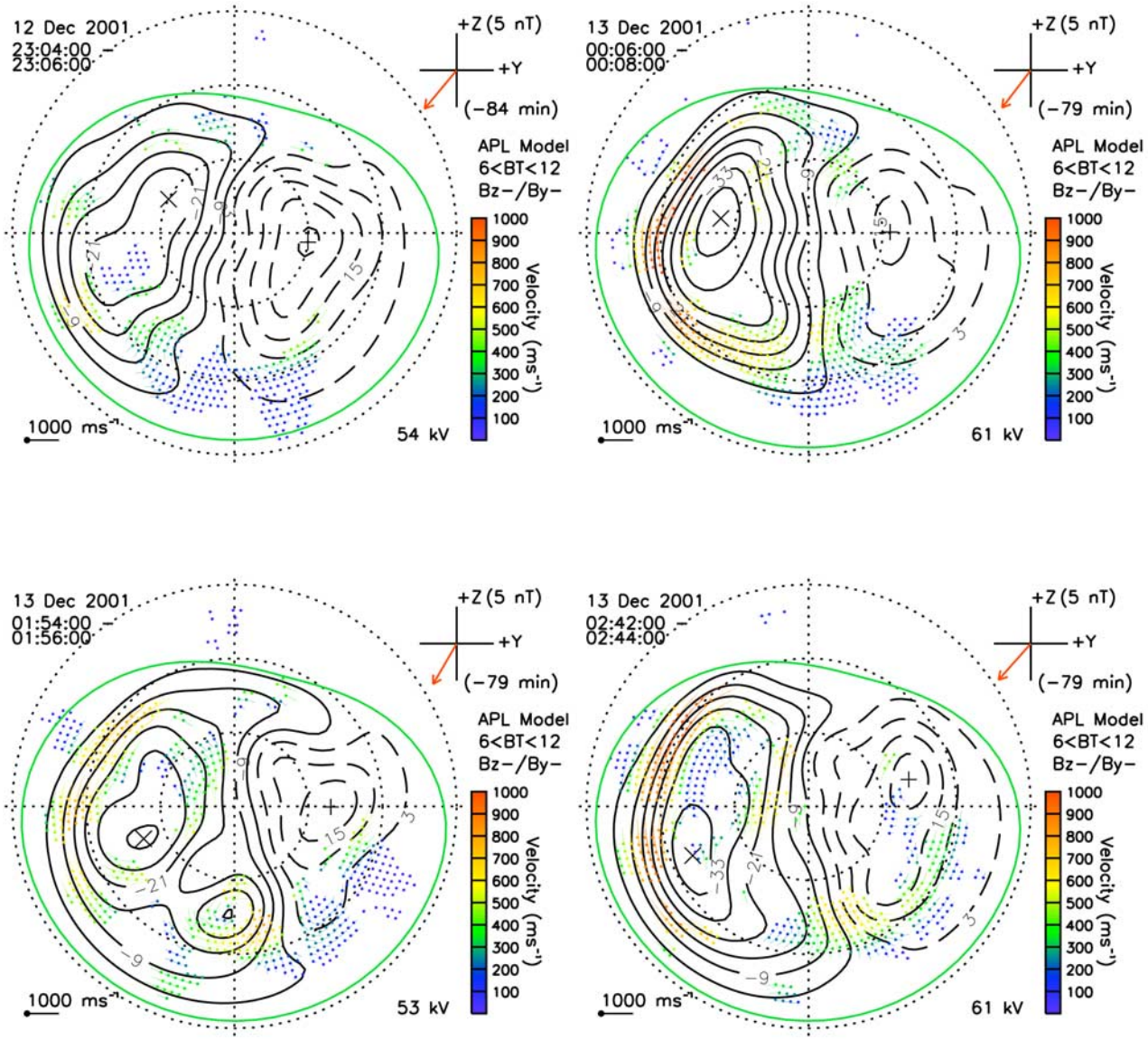

Figure 9. SuperDARN electric potential patterns for the times corresponding to the tomography reconstructions.

Figure 8) the tongue is at its longest, reaching the furthest into the nightside, while the offset of the geographic pole from the geomagnetic pole is toward 06 MLT and the Scandinavian sector is in the correct position to see the enhancement across the lower part of the chain. As time moves on and the geographic pole moves sunward of the magnetic pole, the tongue becomes less intense. The reduction of the TOI is a consequence of less of the convection pattern being in sunlight, although remnants of the enhancement can be seen toward the equatorward extreme of the chain in the final plot at 03 UT.

[22] In order to confirm the choice of convection pattern that was input into the CTIP model, the Super Dual Auroral Radar Network (SuperDARN) electric potential plots were obtained for the same times as the tomographic reconstructions. These are shown in Figure 9 for the four times in question (the plots at 0150 UT and 0156 UT were from the same satellite pass and so too close together to warrant separate SuperDARN plots). The convection pattern input was chosen on the basis of the IMF conditions, but these SuperDARN plots show that it was a good choice, close to the actual conditions. The four examples show cross-polar potentials of 50–60 kV, which is only slightly less than that for the convection pattern chosen for the model to suit the conditions (~76kV, see Figure 3).

5. Discussion

[23] The tomography images from both the Scandinavian and UK chains show an enhancement between 60 and 68 degrees MLAT in the midnight-dawn magnetic sector, suggesting that they are cross-sectional views of the same 'tongue-of-ionization'. Figure 10 shows all the satellite trajectories at the 350 km intersection of the tomographic observations on one polar plot. The location of the peak of the enhancement is shown on each trajectory by a cross.

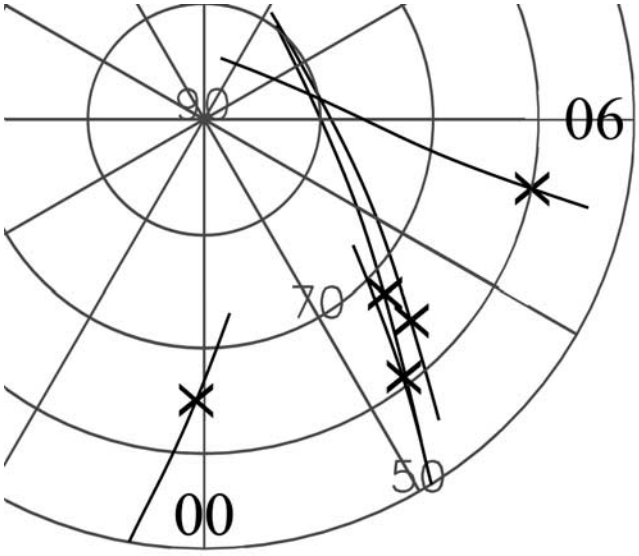

Figure 10. Summary of satellite 350 km intersection trajectories showing relative locations of observed ionization enhancement.

This figure shows that the positions of the feature are broadly in agreement as cross-sections through a continuous feature.

[24] A continuous enhancement in this position would form the poleward wall of the main ionospheric trough; the UK tomographic chain clearly identifies the main trough immediately equatorwards of the enhancement. This, taken in conjunction with the velocity vectors in the SuperDARN plots, suggests that the trough in this case is created by the mechanism suggested by *Rodger et al.* [1992], with the trough being the 'normal' depleted nightside ionosphere flanked by enhancements, which form the walls. This interpretation also fits with the trough being observed at lower latitudes with increasing local time [*Rodger et al.*, 1992; *Pryse et al.*, 2006a]; the position of the enhancement moves slightly equatorward between midnight and dawn.

[25] The EISCAT observations (Figure 6) imply that the enhanced ionization in question was cold, high altitude plasma, which originated upstream and was not created in situ by particle precipitation. To investigate the possible influence of precipitation in maintaining the ionization on the nightside, the model was run again with all the same conditions except that the precipitation energy input was omitted. The results of this run are shown in Figure 11 for each hour between 00 and 03 UT. Comparisons of these results with those of the run shown in Figures 7 and 8 show that there is actually very little difference between the two, including the drawing of the ionization around toward dawn. An equivalent Figure 7 (i.e., latitude versus altitude) plot for the model run without precipitation gives the peak density at 00 UT as 8×10^{11} m^{-3}, which is actually much closer to the observations. Comparisons of the width of the tongue show that the modeled TOI (in both runs) covers a larger latitude range than that observed, but it must be borne in mind that the latitudinal dimension of the grid cells of the model is 2° while that of the observations is 0.25°. It has been shown in other studies comparing CTIP model output to observations [*Pryse et al.*, 2005], that the precipitation input is slightly too high and this would account for the differences in densities between the model run which includes the precipitation and the observations. These predictions, along with the EISCAT results lead us to the conclusion that the in situ precipitation played very little part, if any, in the production of the poleward trough wall observed in this case. The ionization in question must therefore have been created elsewhere. The CTIP model run for these conditions clearly implies that any high-density ionization found in the midnight-dawn sector over Europe, which is in darkness, has been drawn over the polar cap from the dayside by the convection flow.

[26] There have been a few studies showing that photoionization is drawn anti-sunward into the polar cap, perhaps to emerge on the nightside. *Weber et al.* [1984] showed that the source of polar patches was photoionization transported into the polar cap rather than created in situ by precipitation, although their measurements were made at a time of fairly high geomagnetic activity and showed discrete patches and not a tongue. *Pryse et al.* [2004] found that photoionization and convection were also the source of polar cap plasma found near local magnetic noon but separate from the main body of photoionization. In a later study in the dusk-midnight sector, *Pryse et al.* [2006b] used tomography and SuperDARN convection patterns to numerically track a polar patch from the anti-sunward convection flow, through the Harang discontinuity and into sunward flow, where it formed a boundary blob.

[27] Most of these studies have investigated regions of ionization either on the dayside or in the pre-midnight sector. The post-magnetic midnight observations in this study were shown using SuperDARN observations and convection patterns (see Figure 9), to be situated in the dawn cell of the convection. This makes it possible that the observed poleward wall of the main trough in the magnetic midnight-dawn sector originated as photoionization that was drawn over the pole in a tongue-of-ionization and pulled around toward dawn.

[28] So far, only the midnight-dawn sector over Europe has been considered. Model runs include all UTs and so can suggest what may be seen in the midnight-dawn sector over other parts of the Northern Hemisphere. The plots showing the output from the run including both precipitation and convection for every three hours over the 24 h of prediction are presented in Figure 12. The only consistent feature in all plots is the photoionization on the dayside. The plots start at 09 UT to demonstrate the varying shapes and strengths of the tongue-of-ionization. At the beginning of the sequence, there is no tongue-of-ionization. Photoionization is drawn anti-sunward into the convection as the magnetic pole moves sunward of the geographic pole so that more of the convection pattern is in sunlight. The UT dependence, predicted by *Sojka et al.* [1981] due to the offset of the geomagnetic pole and geographic pole, is clearly evident in the changing lengths and thicknesses of the tongue-of-ionization with the change in UT.

[29] *Bowline et al.* [1996] used the Utah State Time-Dependent Ionospheric Model (TDIM) to model the TOI for IMF By positive and negative conditions and its appearance from various single observing sites, including Ny-Ålesund. The TOI was present at most local times above Ny-Ålesund

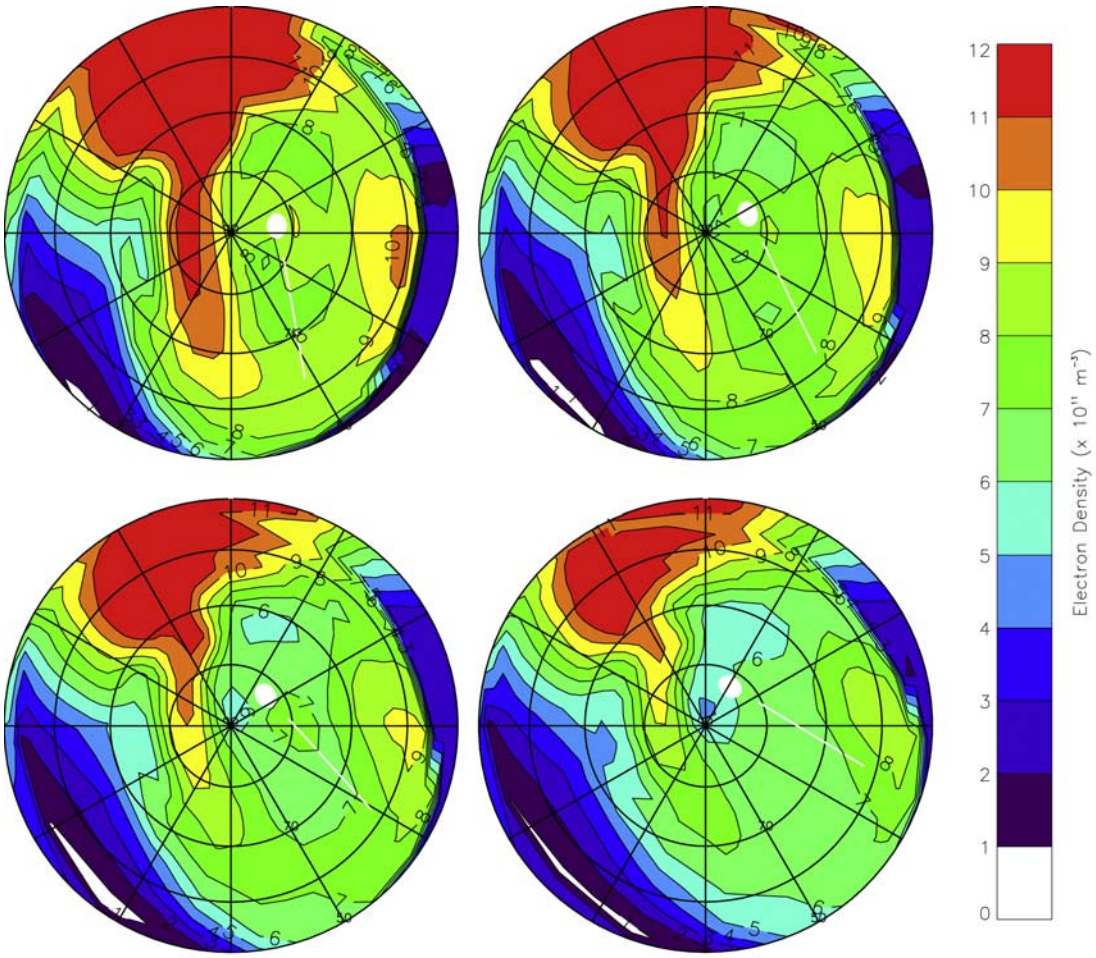

Figure 11. As for Figure 8, with convection turned on but precipitation turned off.

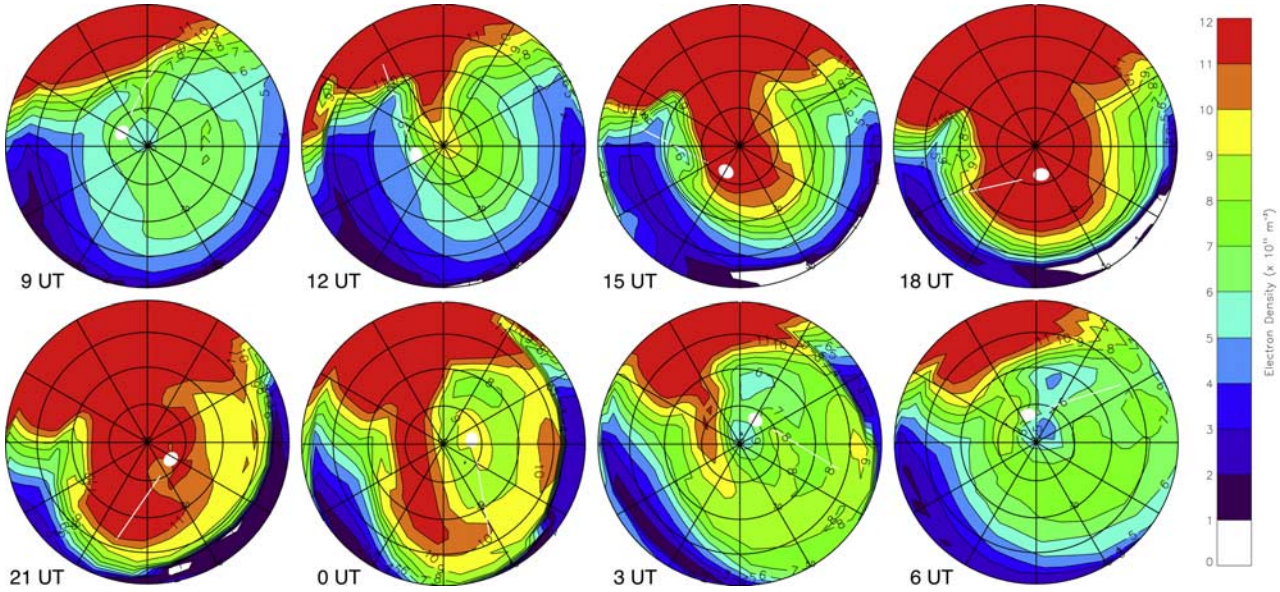

Figure 12. CTIP model results (precipitation and convection were both included) over a whole day, in three-hourly intervals. Note that the sequence begins at 09 UT to highlight the changes in the shape of the tongue of ionization.

with patch-to-background ratios varying between 2 and 5, the lower values occurring around magnetic noon for both By negative and positive. Bowline et al. suggested that the TOI was barely observable at the locality at magnetic noon, although the patch-to-background ratios were around 2. *Pryse et al.* [2004] reported observations by the EISCAT Svalbard radar (ESR) of a weak TOI at magnetic noon with a patch-to-background ratio of about 2.5, larger than the ratio specified by *Crowley* [1996] as necessary to identify a patch. The modeling study of Bowline et al. and the observations of Pryse et al. together with the observations and modeling results from the present study suggest that Svalbard is a particularly good place to see the TOI at nighttime. When Svalbard is at local noon, the offset between the geographic and geomagnetic poles is such that only a small part of the convection is in daylight and little ionization is drawn poleward by the convection. As Svalbard moves to later local times, the offset of the poles brings the convection pattern increasingly into sunlight, and a larger TOI is drawn poleward. On the nightside, at least under the conditions presented in this current study, Svalbard remains under the TOI throughout the midnight-dawn sector as the ionization is swept around toward dawn.

6. Conclusions

[30] There have been relatively few studies of the trough formation in the magnetic midnight-dawn sector. This study suggests that the observed enhancement, forming the poleward edge of the main trough in the midnight-dawn sector, may be dayside photoionization entrained in the convection pattern as a tongue-of-ionization and brought over the polar cap into the nightside. A run of the CTIP model for similar conditions predicts this to be the case. In situ precipitation is thought to be an unlikely source of the ionization due to the plasma being cold and at high altitude (EISCAT measurements) and precipitation is unnecessary to reproduce the tongue-of-ionization across the polar cap in the CTIP model. The model predictions also reveal that under these conditions, the presence of the tongue-of-ionization is heavily UT dependent due to the offset between the magnetic and geographic poles, leading to a situation where the tongue would not be so prominent in observations in the US longitude sector in the midnight-dawn local time sector.

[31] **Acknowledgments.** Financial support for the project was provided by the UK Particle Physics and Astronomy Research Council under grant PPA/G/0/2003/00017. The assistance of the University of Tromsø and the Norwegian Polar Institute in the tomographic measurements are gratefully acknowledged. The SuperDARN radar facility is funded by the National Research Programs of Australia, Canada, Finland, France, Japan, South Africa, Sweden, the UK and the USA and thanks are due to the University of Leicester for providing the data. EISCAT is an international facility supported by the national science councils of China, Finland, France, Japan, Norway and the UK and thanks go to the EISCAT group at the Rutherford Appleton Laboratory for provision of the data. The IMF data were provided by N. Ness (Bartol Research Institute) through CDAWeb.

[32] Wolfgang Baumjohann thanks James Secan and another reviewer for their assistance in evaluating this paper.

References

Bowline, M. D., J. J. Sojka, and R. W. Schunk (1996), Relationship of theoretical patch climatology to polar cap patch observations, *Radio Sci.*, *31*(3), 635–644.

Collis, P. N., and I. Häggström (1988), Plasma convection and auroral precipitation processes associated with the main ionospheric trough at high latitudes, *J. Atmos. Sol. Terr. Phys.*, *50*(4/5), 389–404.

Crowley, G. (1996), Critical review of ionospheric patches and blobs, URSI Review of *Radio Sci.* 1993–1996, edited by W. R. Stone, 619–648.

Evans, J. V., J. M. Holt, W. L. Oliver, and R. H. Wand (1983), The fossil theory of nighttime high latitude F region troughs, *J. Geophys. Res.*, *88*(A10), 7769–7782.

Foster, J. C., J. M. Holt, and R. G. Musgrove (1986), Ionospheric convection associated with discrete levels of particle precipitation, *Geophys. Res. Lett.*, *13*(7), 656–659.

Fuller-Rowell, T. J., and D. Rees (1980), A three-dimensional, time-dependent, global model of the thermosphere, *J. Atmos. Sci.*, *37*, 2545–2567.

Fuller-Rowell, T. J., and D. Rees (1983), Derivation of a conservation equation for mean molecular weight for a two-constituent gas within a three-dimensional, time-dependent, model of the thermosphere, *Planet. Space Sci.*, *32*, 469–480.

Hardy, D. A., M. S. Gussenhoven, and E. Holeman (1985), A statistical model of auroral electron precipitation, *J. Geophys. Res.-Space Phys.*, *90*(NA5), 4229–4248.

Kersley, L., S. Pryse, I. K. Walker, J. A. T. Heaton, C. N. Mitchell, M. J. Williams, and C. A. Willson (1997), Imaging of electron density troughs by tomographic techniques, *Radio Sci.*, *32*(4), 1607–1621.

Knudsen, W. C. (1974), Magnetospheric convection and the high-latitude F2 ionosphere, *J. Geophys. Res.*, *79*(7), 1046–1055.

Moffett, R. J., and S. Quegan (1983), The mid-latitude trough in the electron-concentration of the ionospheric F-layer-A review of observations and modeling, *J. Atmos. Sol. Terr. Phys.*, *45*(5), 315–343.

Muldrew, D. B. (1965), F-layer ionization troughs deduced from Alouette data, *J. Geophys. Res.*, *70*(11), 2635–2650.

Pryse, S. E. (2003), Radio tomography: A new experimental technique, *Surv. Geophys.*, *24*(1), 1–38.

Pryse, S. E., R. W. Sims, J. Moen, L. Kersley, D. Lorentzen, and W. F. Denig (2004), Evidence for solar-production as a source of polar-cap plasma, *Ann. Geophys.*, *22*(4), 1093–1102, SRef-ID: 1432-0576/ag/2004-22-1093.

Pryse, S. E., K. L. Dewis, R. L. Balthazor, H. R. Middleton, and M. H. Denton (2005), The dayside high-latitude trough under quiet geomagnetic conditions: Radio tomography and the CTIP model, *Ann. Geophys.*, *23*(4), 199–206, SRef-ID: 1432-0576/ag/2005-23-1199.

Pryse, S. E., L. Kersley, D. Malan, and G. J. Bishop (2006a), Parameterization of the main ionospheric trouh in the European sector, *Radio Sci.*, *41*(5), RS5S14, doi:10.1029/2005RS003364.

Pryse, S. E., A. G. Wood, H. R. Middleton, I. W. McCrea, and M. Lester (2006b), Reconfiguration of polar-cap plasma in the magnetic midnight sector, *Ann. Geophys.*, *24*(8), 2201–2208.

Quegan, S., G. J. Bailey, R. J. Moffett, R. A. Heelis, T. J. Fuller-Rowell, D. Rees, and R. W. Sprio (1982), A theoretical study of the distribution of ionization in the high-latitude ionosphere and the plasmasphere: First results on the mid-latitude trough and the light-ion trough, *J. Atmos. Terr. Phys.*, *44*(7), 619–640.

Raymund, T. D., S. J. Franke, and K. C. Yeh (1994), Ionospheric tomography: Its limitations and reconstruction methods, *J. Atmos. Sol. Terr. Phys.*, *56*(5), 637–657.

Rodger, A. S., L. H. Brace, W. R. Hoegy, and J. D. Winningham (1986), The poleward edge of the mid-latitude trough-its formation, orientation and dynamics, *J. Atmos. Sol. Terr. Phys.*, *48*(8), 715–728.

Rodger, A. S., R. J. Moffett, and S. Quegan (1992), The role of ion drift in the formation of ionisation troughs in the mid-and high-latitude ionosphere-a review, *J. Atmos. Sol. Terr. Phys.*, *54*(1), 1–30.

Rycroft, J. R., and S. J. Burnell (1970), Statistical analysis of movement of the ionospheric trough and the plasmapause, *J. Geophys. Res.*, *75*(28), 5600–5604.

Sojka, J. J., W. J. Raitt, and R. W. Schunk (1981), A theoretical study of the high-latitude F region at solar minimum for low magnetic activity, *J. Geophys. Res.*, *86*(A2), 609–621.

Weber, E. J., J. Buchau, J. G. Moore, J. R. Sharber, R. C. Livingston, J. D. Winningham, and B. W. Reinisch (1984), F layer ionization patches in the polar cap, *J. Geophys. Res.*, *89*(NA3), 1683–1694.

R. Balthazor, US Air Force Academy, Department of Physics, Suite 2C12, 2354 Fairchild Drive, Colorado Springs, CO 80840, USA.

H. R. Middleton, S. E. Pryse, and A. G. Wood, Institute of Mathematical and Physical Sciences, University of Wales Aberystwyth, Aberystwyth, SY23 3BZ, United Kingdom. (hrm@aber.ac.uk)